Magnetic Skyrmion-based Neural Recording System Design for Brain Machine Interface

Biao Pan*, Kang Wang†, Xing Chen†, Jinyu Bai†, Jianlei Yang‡, Sai Li†, Youguang Zhang* and Weisheng Zhao†

Email: {mingren200323, wang.kang, xing.chen0118, 13021042, jianlei, saili, zyg, weisheng.zhao}@buaa.edu.cn

*School of Electronic and Information Engineering, Beihang University, Beijing 100191, China.

†School of Microelectronics, Beihang University, Beijing 100191, China.

‡School of Computer Science and Engineering, Beihang University, Beijing, 100191, China.

***Abstract*—Next-generation brain machine interface demand a high-channel-count neural recording system to wirelessly monitor activities of thousands of neurons. In order to achieve high-density neural recording, further development of single recording channel comprised of a neural amplifier front-end (AFE) and an analog-to-digit converter (ADC) is critical. Despite the great progress made in CMOS implementation of custom-designed neural recording system, hybrid limitations of increasing area and power consumption in line with Moore's law drove great demand for post-CMOS substitutes. Magnetic skyrmion with nano particle-like and non-volatile properties are of both fundamental and applied interests for future bio-inspired electronics. In this work, we propose a compact model including both AFE and ADC based on current-induced skyrmion motion. The proposed system achieved a power consumption of 0.63 pJ/channel with an area overhead of 0.14 μm^2. The purpose of this work is to explore the feasibility of magnetic skyrmion for building large-scale, dense neuronal recording system which could pave a new way for future brain machine interface application.**

Keywords—Skyrmion, Brain Machine Interfaces, AFE, ADC, Neural recording.

I. Introduction

Brain machine interfaces (BMI) hold great promise to restore motor and sensory functions for patients suffering from neurological disorders [1-3]. Since the first experimental demonstration in 1999 that ensembles of cortical neurons could directly control a robotic manipulator, basic research on BMI has moved at a stunning pace [4]. To enable future BMI for prosthetics with high degrees of freedom and natural movement dexterity, it is a general consensus that thousands of neurons distributed in multiple neuronal ensembles be monitored simultaneously [5][6]. In decades of BMI research, multi-channel neural recording system (NRS) are increasingly applied for facilitating the record of the neurophysiological behavior of the human brain [7].

Each recording channel of NRS is usually composed of two distinct functional blocks: a neural amplifier front-end (AFE) to gain the weak neural signals that are transduced through electrode interfaces and a low power analog-to-digit converter (ADC) to digitize neural signals [8]. AFE and ADC have conventionally been designed and fabricated using the application specific integrated circuit (ASIC) solution, constituting CMOS based neurochips [9]. Several research groups have recently demonstrated CMOS based NRS to acquire untethered and portable neural recordings in BMI applications [10][11]. However, CMOS implementation face two challenges: noise-versus-power tradeoff and large area overhead. On one hand, neural signals are typically susceptible to inherent noise of the electronic components and external sources of interference include unwanted biopotential signals. Existing AFE circuits typically have unacceptable noise level or consume too much power to be fully implanted in large quantities [12]. On the other hand, integrating ADCs in every channel need large area of analog circuits which is exacerbated by poor scaling of analog circuits in CMOS due to quantum effects in advanced technologies [13]. These decrease the attraction of CMOS ASIC to wireless neural recording devices and arouse for post-CMOS non-volatile implementation.

Magnetic skyrmions are localized and topologically protected spin configurations, which can be stabilized by Dzyaloshinskii-Moriya interactions (DMIs) in chiral bulk magnets or in thin films with broken inversion symmetry [14]. With the salient features of nanoscale size, high drifting velocity as well as non-volatile memory property, skyrmion has emerged as a prospective information carrier in the future ultra-dense, high-speed, and low power bio-electronics [15]. Recently, a hybrid model enabling the information transmission between a skyrmion and domain-wall (DW) device which make the high-quality amplification of weak signals possible was established and verified by the experiments [16][17]. Moreover, current-induced skyrmion motion has driven the invention of skyrmion-based racetrack (Sky-RM) that hold promise for non-volatility, high density, and low power ADC [18]. These studies indicated that intrinsic properties of the emerging skyrmion might help tackle challenges in NRS design for BMI while further research is still needed to confirm this assumption.

In this work, a compact full-skyrmion based recording channel model is proposed in order to simultaneously minimized power consumption, area overhead and improve signal conditioning. To carefully design and perform neural signal recording, we employed an AFE made of skyrmions and DW that are specifically designed to amplify spike signals and a n-bit Sky-RM structure using magnetic nanotracks as ADC to realize differential input with single-ended digital output.

This work was supported by the China Postdoctoral Science Foundation (2018M640044) and the National Natural Science Foundation of China (61871008).

978-1-7281-0397-6/19/$31.00 ©2019 IEEE

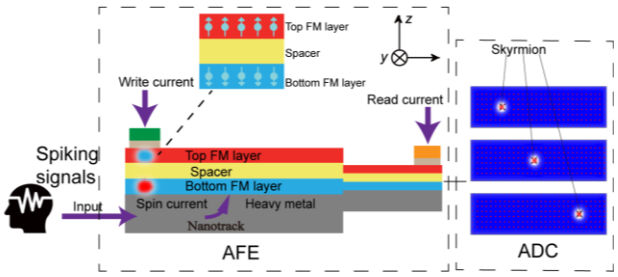

Fig.1. Schematic illustration of the proposed multichannel neural recording architectures with every channel consiting of an individual AFE and ADC.

Finally, micromagnetic and hybrid circuit simulations were performed to evaluate the energy and area performance. We hope that this preliminary research will be the basis of skyrmion based NRS and promote the development of skyrmion from fundamental physics to realistic electronics in next generation BMI application.

This paper is organized as following: Section II describes the signal transmission in the proposed system and single channel modeling of skyrmion based AFE and ADC block for neural recording. In Section III, micromagnetic and circuit simulation methods were employed to carefully depict the signal processing and analyze the power and area performance of single channel. Section IV summarizes the work.

II. Technology Modeling And System Design

The overall architecture and building block design of skyrmion based NRS in this work were illustrated in Fig. 1. With multi-electrode implants employing individually movable microwire bundles have been proved experimentally feasible [19], we employed N-channel integrated system to record the activity of neuronal ensembles simultaneously. Each channel consists of a skyrmion-DW AFE to amplify the spike signal without unexpected noise and a Sky-RM ADC to convert the analog signal to digital output. The primary component of the NRS is a bilayer nanotrack (see Fig. 1), along which a skyrmion can move back and forth driven by an electrical current pulse flowing through the heavy metal under the nanotrack via the spin Hall effect. The bilayer nanotrack, which consists of a top ferromagnetic (FM) layer and a bottom FM layer separated by an insulating spacer layer, has a linear perpendicular magnetic anisotropy.

A. Skyrmion-DW AFE

As shown in Fig.2, the conversion process from a skyrmion to a DW pair on a junction comprised of a wide nanotrack on the left side and a narrow nanotrack on the right side was described in detail. At time t_1, a skyrmion is initially nucleated and then move forward along the nanotrack under the driving current. During this process, the skyrmion will not move unless the driving current density exceeds the depinning current density which means the skyrmion motion acts as the role of filter to remove low-intensity noise and extract valid signal effectively. Such property is fundamental to construction of a low-noise AFE and will be proved in section III. When the skyrmion reaches the junction interface at t_2, the continuity of the skyrmion spin texture is destroyed and the topological number Q continuously change from 1 to 0. Finally, skyrmion is converted to DW pair at t_3.

The skyrmion and domain wall can be detected by a MTJ In our read head model, we consider the tunnel magnetoresistance (TMR) effect for skyrmion detection with a perpendicularly polarized MTJ device. In the presence of a skyrmion, the site-dependent spin mixing of the magnetic states will be modified owing to the noncollinear spin textures as compared with the ferromagnetic background. Therefore, a drastic change occurs in the differential tunneling conductance (or resistance), therefore making a skyrmion distinct from the ferromagnetic background [20], in which the resistance can be expressed as (1):

$$R = \frac{2}{G_P+G_{AP}+(G_P-G_{AP})cos\theta} \qquad (1)$$

with G_P and G_{AP} corresponding to the relative magnetizations parallel (P, θ =0°) and antiparallel (AP, θ =180°) of the ferromagnetic layers, respectively. For DW, the value of $cos\theta$ can be varied from -1 to 1, while in skyrmion case, the value range is smaller due to the hedgehog or spiral configurations of a skyrmion. Thus, compared to skyrmion, the readout of DW signal is more powerful as it makes use of all the fully reversed spins which is the original reason for signal amplification. Moreover, a precise control of the time sequence of multi-skyrmions is possible by controlling the magnetic field to create a sequence of DW pairs without extra electronic devices. Therefore, such skyrmion-DW AFE device has the advantages as low-noise amplifier of weak neural signals in NRS channel getting rid of both inherent and external noise.

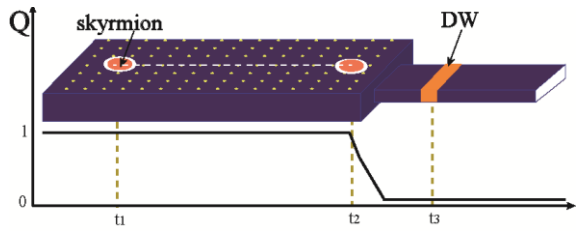

Fig.2. Conversion between a skyrmion and a DW pair: a skyrmion is converted into a DW pair driven by injected current from the wide part to the narrow part of the nanowire. The topological number Q will also change from 1 to 0 come along with the skyrmion to DW change.

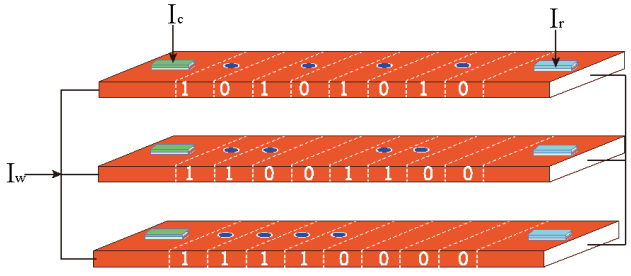

Fig.3. Structure of a Sky-RM based 3bit converter with 3 nanotracks. Each nanotrack is configured with different distribution of skyrmions and represents an individual bit.

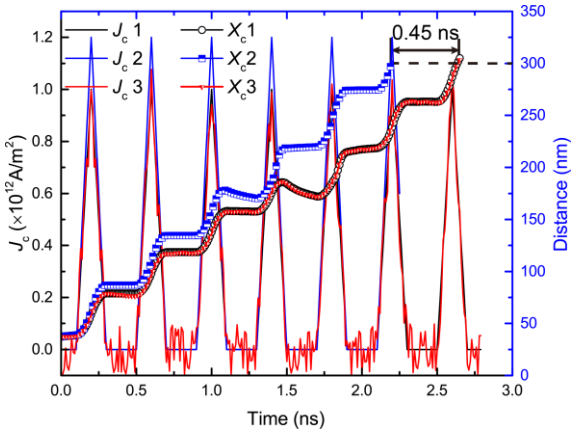

Fig.4. The skyrmion moving distance under different kinds of input current signals.

B. *Sky-RM ADC*

To illustrate the potential adoption of the Sky-RM ADC into NRS channel, the working principle of 3bit Sky-RM ADC was described in Fig. 3. A 3-bit Sky-RM ADC requires 3 components each is composed of four skyrmions, a write head for skyrmion creation, a nanotrack for skyrmion motion, a read head for skyrmion detection and peripheral CMOS circuits for generating the skyrmion creation current (I_c), reading current (I_r) and writing current (I_w). Each nanotrack will be configured differently such that each generates a single bit, from LSB to MSB. Then, the binary data information (i.e., "0" or "1") is encoded by the absence or presence of a skyrmion.

The overall converter operation can be conducted in the following four stages:

1) Initialization: the skyrmions are initially created by injecting spin-polarized current I_c through the write head, depending on the bit width and are then moved along the nanotrack to specified position by the spin driving current;

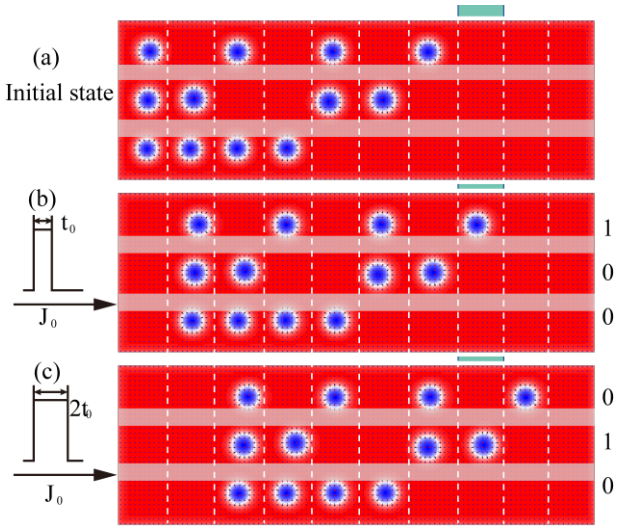

Fig.5. Micromagnetic simulation results of the skyrmion based ADC model. (a) Initial state of the skyrmions in ADC converter. Note here the light red areas separating the three tracks have a higher PMA constant (K_u=0.9 MJ · m^{-3}) to form energy barriers, which can be achieved by the voltage controlled magnetic anisotropy method.

2) Conversion: after initialization, the same input current I_w from the signal source is injected into the nanotrack. After time t, the analog input current will be converted to digital output depending on the distance X_c of the skyrmions movement.

3) Read: the skyrmion can be detected by applying a detection current (I_r) through the read MTJ because of the tunnel magneto-resistance (TMR) effect. Therefore, a 0 or 1 state of each nanotrack can be determined and the input analog current data has been converted to digital output;

4) Reset: in the interval of two conversion, a reset operation is required. Horizontal reset current flows through the nanotrack to cause skyrmion move back to their original position to be prepared for the next signal arrived.

III. Results And Discussion

In this section, micromagnetic and circuit simulation methods are employed to carefully analyze the proposed skyrmion NRS. The relevant parameters and experiment design employed to implement the micromagnetic and circuit simulations are also discussed. Despite that the individual nanotrack between adjacent tracks can be segregated by various methods, for example, by physical separation or by constructing barriers, we adopt the latter one for micromagnetic simulations in this work.

A. *Micromagnetic Simulation*

The micromagnetic simulations are performed by solving the Landau-Lifshitz-Gilbert (LLG) equation (Eq. (2)) on the platform of the Object Oriented Micro Magnetic Framework (OOMMF) [21][22].

$$\frac{dm}{dt} = -\gamma m \times h_{\text{eff}} + \alpha\left(m \times \frac{dm}{dt}\right) - \frac{\gamma \hbar P j_d}{2\mu_0 e M_s t_f}\left[m \times \left(m \times m_p\right)\right] \qquad (2)$$

where $h_{\text{eff}} = H_{\text{eff}}/M_S$ denotes the reduced effective field, which includes all the magnetic field contributions, such as the demagnetization filed, the exchange field, the anisotropy field, and the DMI field. $M_S = |m|$ is the saturation magnetization, α is the Gilbert damping factor, γ is the gyromagnetic ratio, $\hbar$ is the reduced Planck constant, P is the spin polarization, e is the

TABLE I. KEY PARAMETERS USED IN MICROMAGNETIC SIMULATIONS

Sat. magnetization, M_s	$580\ kA \cdot m^{-1}$
Gilbert damping, α	0.3
Exchange stiffness, A	$15\ pJ \cdot m^{-1}$
DMI constant, D	$3.5\ mJ \cdot m^{-2}$
PMA constant, K_u	$0.8\ MJ \cdot m^{-3}$
Spin polarization rate, P	0.4
Driving current density, J_0	$6 \times 10^{11}\ A/m^2$

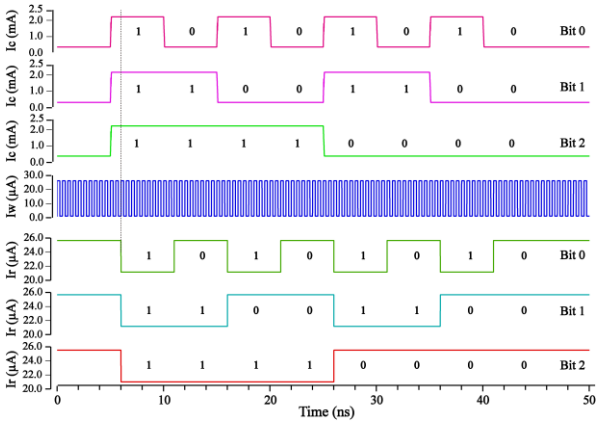

Fig.6. Transient simulation waveforms of the Sky-RM ADC for different track.

electron charge, j_d is the driving current density, μ_0 is the vacuum permeability, t_f is the thickness of the nanotrack. More details on the micromagnetic simulations can refer to [23][24].

The micromagnetic simulation results of skyrmion-DW AFE and Sky-RM ADC are illustrated in Fig. 4 and Fig. 5, respectively. As shown in Fig.4, the two different input signals without noise $J_c1 = 1 \times 10^{12}$ A/m^2, $J_c2 = 1.2 \times 10^{12}$ A/m^2 and skyrmion motion under them were signified by the black and blue curve, respectively. From the comparison of these two curves, there exists a clear positive correlation between J_c and X_c. Furthermore, as the random noise with a maximum amplitude of 10% of the desired signal was introduced into the J_c1 to form J_c3, the trajectory of X_c3 (red curve) is nearly the same as the X_c1 indicated the anti-noise characteristic of the proposed skyrmion-DW model.

As shown in Fig.5, the input current under measurement flows through the nanotrack in the opposite direction of the reset current. In this case, all skyrmions move to right simultaneously. As the current under measurement for each nanotrack has the same value, the skyrmions in different nanotracks move at the same velocity. Durations t_0 in (a) and $2t_0$ in (b) of the current J_0 are applied to the converter device respectively, leading to the digital outputs as "1" (001), "2" (010), respectively.

TABLE II. CALCULATION OF THE ENERGY CONSUMPTION AND AREA OVERHEAD

Parameters	**AFE**	**ADC**
Width (nm)	60	200
Length (nm)	400	600
Area (μm^2)	0.14	
Resistance (kΩ)	3.00	1.35
Current (mA)	0.04	0.48
Power (pJ)	0.01	0.62*
Total Power (pJ)	0.63	

**average power consumption of digital output 0-7*

B. Circuit Simulation

Based on the 3bit Sky-RM ADC model, we performed hybrid skyrmion/CMOS simulations on the Cadence design platform to demonstrate the circuit performance and calculate the power consumption. The transient simulation waveforms were shown in Fig.6.

Under the I_c of 2.03 mA, provided by the spin-valve write head, the binary data of bit-0 (10101010), bit-1(11001100) and bit-2(11110000) are encoded by the absence or presence of a skyrmion and written into the nanotrack. Then the skyrmion was driven by the driving current I_w of 27.85μA with pulse duration of 0.2ns to move along the nanotrack. During the motion, the skyrmion can be pinned by the repulsive force from the nanotrack edge, we can design the lowest depinning current to compensate the threshold current of skyrmion motion. Finally, the skyrmions reach the MTJ read head (see Fig. 5) and are detected by measuring the conductance change. As the conductance will decrease when a skyrmion is detected, the detection current is I_r of 25.13μA or 20.87μA for the absence or presence of a skyrmion.

In order to assert the superiority of the skyrmion over the CMOS analogues, the energy and area performance were calculated and listed in Table II. The power efficiency of the nanotrack could be calculated by the product of square of current and the resistance of the nanotrack. As the current density and resistivity have been set within the simulation, the current could be easily obtained. Considering the average motion duration of the skyrmions in the nanotrack, the power consumption of the AFE and ADC were calculated as 0.01pJ and 0.62pJ, respectively. Meanwhile, the area overhead of each channel was estimated by calculated the total area of all the nanotracks to be 0.14 μm^2. All of these figures are of great superiority to facilitate miniaturization of NRS in BMI.

IV. CONCLUSION

In conclusion, we propose a full skyrmion based neural recording channel for NRS design. The overall performance evaluated through micromagnetic and circuit simulation shows that the proposed system can efficiently complete signal amplification and digitalize task in an energy and area saving manner. Despite its limitations, this preliminary result suggests new possibilities for utilization of skyrmion for neural recording and will encourages us on promoting skyrmion-based devices in more complex BMI applications.

REFERENCES

[1] M. A. Lebedev, M. A. Nicolelis. "Brain-Machine Interfaces: From Basic Science to Neuropro-stheses and Neurorehabilitation," *Physiological Reviews*, vol. 97, no. 2, pp. 767-837, 2017.

[2] M. D. Serruya, N. G. Hatsopoulos, L. Paninski, M. R. Fellows and J. P. Donoghue. "Instant neural control of a movement signal," *Nature*, vol. 416, pp. 141-142, 2002.

[3] M. A. Lebedev, M. A. L Nicolelis. "Brain-machine interfaces: past, present and future," *Trends Neurosci*, vol. 29, no. 9, pp. 536-546, 2006.

[4] J. K. Chapin, et al. "Real-time control of a robot arm using simultaneously recorded neurons in the cortex," *Nat. Neurosci*, vol. 2, pp. 664-670, 1999.

[5] A. N. Belkacem, S. Nishio, T. Suzuki, H. Ishiguro and M. Hirata, "Neuromagnetic Decoding of Simultaneous Bilateral Hand Movements for Multidimensional Brain-Machine Interfaces," *IEEE Transactions on Neural Systems and Rehabilitation Engineering*, vol. 26, no. 6, pp. 1301-1310, 2018.

[6] G. N. Angotzi et al., "A Synchronous Neural Recording Platform for Multiple High-Resolution CMOS Probes and Passive Electrode Arrays," *IEEE Transactions on Biomedical Circuits and Systems*, vol. 12, no. 3, pp. 532-542, 2018.

[7] R. Chen, A. Canales and P. Anikeeva. "Neural recording and modulation technologies," *Nature Reviews Materials*, vol. 2, no. 2, pp. 16093, 2017.

[8] J. Scholvin, C. G. Fonstad and E. S. Boyden, "Scaling models for microfabricated in vivo neural recording technologies," *2017 8th International IEEE/EMBS Conference on Neural Engineering (NER)*, Shanghai, pp. 181-185, May. 2017.

[9] R. R. Harrison and C. Charles, "A low-power low-noise CMOS amplifier for neural recording applications," *IEEE Journal of Solid-State Circuits*, vol. 38, no. 6, pp. 958-965, June. 2003.

[10] S. Lee, A. J. Cortese, et al., "A 330μm×90μm opto-electronically integrated wireless system-on-chip for recording of neural activities," *2018 IEEE International Solid - State Circuits Conference - (ISSCC)*, San Francisco, CA, pp. 292-294, 2018.

[11] C. Kim, S. Joshi, et al., "A 92dB dynamic range sub-μVrms-noise 0.8μW/ch neural-recording ADC array with predictive digital autoranging," *2018 IEEE International Solid - State Circuits Conference - (ISSCC)*, San Francisco, CA, pp. 470-472, 2018.

[12] X. Tong and M. Ghovanloo, "Multichannel Wireless Neural Recording AFE Architectures: Analysis, Modeling, and Tradeoffs," *IEEE Design & Test*, vol. 33, no. 4, pp. 24-36, Aug. 2016.

[13] X. Li, B. Taylor, Y. T. Chien and L. T. Pileggi, "Adaptive post-silicon tuning for analog circuits: concept, analysis and optimization," *2007 IEEE/ACM International Conference on Computer-Aided Design*, San Jose, CA, pp. 450-457, 2007.

[14] J. Sampaio, V. Cros, S. Rohart, A. Thiaville and A. Fert, "Nucleation, stability and current-induced motion of isolated magnetic skyrmions in nano-structures", *Nature Nanotechnology*, vol. 8, no. 11, pp. 839-844, 2013

[15] X. Chen, W. Kang et al., "A Compact Skyrmionic Leaky-integrate-fire Spiking Neuron Device," *Nanoscale*, vol. 10, no. 13, pp. 6139-6146, 2018

[16] W. Jiang, P. Upadhyaya, et al., "Blowing magnetic skyrmion bubbles", *Science*, vol. 349, no. 6245, 2015.

[17] Y. Zhou and M. Ezawa, "A reversible conversion between a skyrmion and a domain-wall pair in a junction geometry", *Nature Communications*, vol. 5, no. 4652, Aug 2014.

[18] W. Kang et al., "Compact Modeling and Evaluation of Magnetic Skyrmion-Based Racetrack Memory," *IEEE Transactions on Electron Devices*, vol. 64, no. 3, pp. 1060-1068, Mar 2017.

[19] G. Buzsáki, "Large-scale recording of neuronal ensembles," *Nature Neuroscience*, vol. 7, no. 5, pp. 446-451, 2004.

[20] C. Hanneken et al., "Electrical detection of magnetic skyrmions by tunnelling non-collinear magnetoresistance," *Nature Nanotechnol.*, vol. 10, no. 12, pp. 1039-1042, 2015.

[21] S. H. Yang, S. Parkin. "Domain-Wall Velocities of up to 750 M/S Driven by Exchange-coupling Torque in Synthetic Antiferromagnets." *Nature. Nanotechnology*, vol. 10, no. 3, pp. 221-226. 2015.

[22] M. J. Donahue, and D. G. Porter. "OOMMF User's guide." *National Institute of Standards and Technology*, Interagency Report, Gaithersburg, Jan. 1999, Online. Available: http://math.nist.gov/oommf

[23] X. Zhang, Y. Zhou, and M. Ezawa, Magnetic bilayer-skyrmions without skyrmion hall effect, *Nature Comm.*, vol. 7, no. 10293, pp. 1-7, 2016.

[24] W. Kang et al., "Complementary skyrmion racetrack memory with voltage manipulation," *IEEE Electron Device Lett.*, vol. 37, no. 7, pp. 924-927, 2016.